Closed-form solution of the convolution integral in the magnetic resonance dispersion model for quantitative assessment of angiogenesis

S. Turco, A.J.E.M. Janssen, C. Lavini, J.J. de la Rosette, H. Wijkstra, and M. Mischi

Abstract— **Prostate cancer (PCa) diagnosis and treatment is still limited due to the lack of reliable imaging methods for cancer localization. Based on the fundamental role played by angiogenesis in cancer growth and development, several dynamic contrast enhanced (DCE) imaging methods have been developed to probe tumor angiogenic vasculature. In DCE magnetic resonance imaging (MRI), pharmacokinetic modeling allows estimating quantitative parameters related to the physiology underlying tumor angiogenesis. In particular, novel magnetic resonance dispersion imaging (MRDI) enables quantitative assessment of the microvascular architecture and leakage, by describing the intravascular dispersion kinetics of an extravascular contrast agent with a dispersion model. According to this model, the tissue contrast concentration at each voxel is given by the convolution between the intravascular concentration, described as a Brownian motion process according to the convective-dispersion equation, with the interstitium impulse response, represented by a mono-exponential decay, and describing the contrast leakage in the extravascular space. In this work, an improved formulation of the MRDI method is obtained by providing an analytical solution for the convolution integral present in the dispersion model. The performance of the proposed method was evaluated by means of dedicated simulations in terms of estimation accuracy, precision, and computation time. Moreover, a preliminary clinical validation was carried out in five patients with proven PCa. The proposed method allows for a reduction by about 40% of computation time without any significant change in estimation accuracy and precision, and in the clinical performance.**

I. INTRODUCTION

Angiogenesis plays a fundamental role in cancer growth and the development of metastasis [1], [2]. In cancer, angiogenesis leads to the formation of a dense network of tortoise and leaky microvessels in a poorly organized vascular environment, exhibiting increased arteriovenous shunts and chaotic flow patterns. Novel cancer therapies aimed at inhibiting angiogenic processes and/or disrupting angiogenic tumor vasculature are currently being developed and tested [3]. Focal therapies for localized cancers are also available [4], [5], but accurate cancer delineation is required for their efficient use. The need for early evaluation and monitoring of therapeutic response to angiogenic treatment, and for earlier and improved cancer localization, has led to the development of several dynamic contrast-enhanced (DCE) imaging methods for *in-vivo* non-invasive assessment of tumor angiogenesis [6], [7], [8], [9], [10].

In DCE magnetic resonance imaging (MRI), the adopted contrast agent leaks across the vascular endothelium into the intersitium. Assessment of the contrast agent distribution between the intravascular and extravascular spaces offers the opportunity to investigate the functional and structural changes in tumor vasculature. To this end, pharmacokinetic models are fitted to contrast concentration time curves (CTCs) measured at each voxel by DCE-MRI, leading to the estimation of quantitative parameters that are related to the physiology underlying tumor angiogenesis [7], [10], [11].

Recently, magnetic resonance dispersion imaging (MRDI) has been proposed as a new method to characterize the changes in the tumor microvasculature, by assessing the intravascular dispersion kinetics of an extravascular contrast agent with a dispersion model [10]. A preliminary validation of this method for prostate cancer (PCa) localization has shown promising results, encouraging further research.

The clinical relevance of PCa is confirmed by the most recent statistics. It accounts for 27% of estimated new cancer cases and 10% of estimated cancers deaths in males, in the Unites States [12]. Current diagnosis of PCa still relies on repeated systematic biopsies, hampering the efficient and timely use of the available focal therapies [13], [14], and evidencing a need for imaging methods enabling reliable PCa localization.

MRDI can reveal the presence of cancer neo-angiogenesis by generating parametric maps related to the microvascular architecture (dispersion parameter, κ) and to the microvascular permeability (leakage parameter, k_{ep}). Parameter estimation is obtained by fitting CTCs measured with DCE-MRI by the proposed dispersion model. According to this model, the tissue contrast concentration at each voxel is given by the convolution between the intravascular concentration, described as a Brownian motion process according to the convective-dispersion equation, with the interstitium impulse response, represented by a mono-exponential decay, and describing the contrast leakage in the extravascular space.

Due to the non linear nature of the model, parameter estimation is performed by an iterative fitting routine which minimizes an objective function given by the sum of squared errors. The presence of the convolution integral increases the computational burden of the fitting routine by introducing N^2 multiplications at each iterative step, where N is the number of time samples in the CTC.

Based on the promising results obtained by MRDI for prostate cancer localization, in this work an improved formu-

*This work was supported by the European Research Council (ERC)

S. Turco, H. Wijkstra, and M. Mischi are with the Department of Electrical Engineering, Eindhoven Univeristy of Technology, 5612 AZ Eindhoven, The Netherlands. s.turco@tue.nl

A.J.E.M. Janssen is with the Department of Mathematics and Computer Science, Eindhoven Univeristy of Technology, 5612 AZ Eindhoven, The Netherlands.

C. Lavini, J.J. de la Rosette, H. Wijkstra are with the Academic Medical Center, University of Amsterdam, 1105 AZ Amsterdam, The Netherlands.

lation of the dispersion model is proposed and tested in PCa. The new formulation is obtained by providing a closed-form solution of the convolution integral present in the dispersion model. A closed-form solution is attractive because it may improve the time performance of the parameter estimation method by reducing the number of operations to be performed at each step of the iterative fitting routine. Moreover, the shape of the objective function is also changed, leading to possible reduction in the estimation error. The performance of the proposed solution is tested by dedicated simulations, and compared in terms of estimation computation time, accuracy, precision and robustness to noise. Moreover, a preliminary clinical evaluation is carried out on five patients with proven PCa.

II. THEORY

A. Extravascular contrast-agent dispersion modeling

The concentration of an extravascular contrast agent in a voxel of tissue is given by the weighted sum of the intravascular and the extravascular concentrations as

$$C_t(t) = v_p C_p(t) + v_e C_e(t), \tag{1}$$

where $C_t(t)$ is the tissue contrast concentration, $C_p(t)$ and $C_e(t)$ are the plasma and extravascular concentrations, respectively, and v_p and v_e are the plasma and extravascular fractional volumes, respectively. The leakage of the contrast agent from the intravascular space into the interstitium can be described by the model of Tofts et al. [11] as a transport process driven by the concentration gradient,

$$v_e \frac{\partial C_e(t)}{\partial t} = K^{trans}(C_p(t) - C_e(t)), \tag{2}$$

where K^{trans} represents the volume transfer constant. Assuming negligible contribution of the plasma compartment (i.e. $v_p \simeq 0$), and solving (2) with initial conditions $C_e(0) = C_t(0) = 0$, the contrast concentration at each voxel is described as

$$C_t(t) = K^{trans} C_p(t) * e^{-k_{ep}t}, \tag{3}$$

where $k_{ep} = K^{trans}/v_e$ is the black-flux rate from the extravascular space into the blood plasma, and the symbol $*$ represents the convolution integral.

The contrast kinetic in the intravascular phase in a voxel of tissue can be modeled as a Brownian motion process, described by the convective-dispersion equation. A solution of this equation is given by the modified local density random walk model, which provides a local characterization of the dispersion process as [9]

$$C_p(t - t_0) = \alpha \sqrt{\frac{\kappa}{2\pi(t-t_0)}} e^{-\frac{\kappa(t-\mu-t_0)^2}{2(t-t_0)}}, \tag{4}$$

with α being the time-integral of $C_p(t)$, t_0 being the theoretical contrast injection time, μ being the mean transit time of the contrast particles between injection and detection sites, and κ being the intravascular dispersion parameter, given by the local ratio between contrast convection (squared velocity v^2) and dispersion (dispersion coefficient D). In the presence of convection through a microvascular network, dispersion is mainly determined by the multipath trajectories across the microvascular bed. For these reasons, the local dispersion parameter has been adopted to characterize the microvascular architecture [9].

By making the adiabatic approximation [15], which assumes the kinetics of the intravascular dispersion to be much faster than the extravascular leakage (i.e. $\kappa \gg k_{ep}$), the intravascular concentration $C_p(t)$ in (3) can be substituted by $C_p(t)$ given in (4). The resulting dispersion model is thus obtained as

$$C_t(t - t_0) = A \left(\sqrt{\frac{\kappa}{2\pi(t-t_0)}} e^{-\frac{\kappa(t-\mu-t_0)^2}{2(t-t_0)}} \right) * \left(e^{-k_{ep}t} \right). \tag{5}$$

with $A = K^{trans}\alpha$.

B. Closed-form solution of the convolution integral

A closed-form solution of (5) is obtained as

$$\begin{aligned} C_t(t) =& A\sqrt{\frac{\kappa}{8z}} e^{-k_{ep}(t-t_0)+\kappa\mu} \times \\ & [e^{2\sqrt{z\varpi}}(erf(\sqrt{zt} + \sqrt{\varpi/t}) - 1) + \\ & e^{-2\sqrt{z\varpi}}(erf(\sqrt{zt} - \sqrt{\varpi/t}) + 1)]. \end{aligned} \tag{6}$$

where erf represents the error function, and the following substitutions have been made:

$$\begin{cases} z = \frac{1}{2}\kappa - k_{ep} \\ \varpi = \frac{1}{2}\kappa\mu^2 \end{cases}, \tag{7}$$

with the condition $\kappa > 2k_{ep}$, in accordance with the adiabatic approximation. A more detailed derivation of (6) can be found in the appendix.

III. METHODS

A. Simulations

The performance of the novel method (Eq. (6)) were compared with the original method (Eq. (5)) in terms of estimation time, accuracy, precision and robustness to noise. A simulated data-set of 1375 clean CTCs was obtained by simulating the partial differential equation in (2) in a finite-difference approach, with intravascular concentration as in (4). The parameters were changed within the ranges $0.005 \div 4$ s^{-1}, for κ, and $0.005 \div 6$ min^{-1}, for k_{ep}, according to the values found in literature [9], [16], and with additional condition, due to the adiabatic approximation, of $\kappa > 2k_{ep}$.

The effect of noise was evaluated by adding to the simulated CTCs Gaussian noise with standard deviation $\sigma = CTC_{peak}/10^{SNR}$, with CTC_{peak} being the maximum of the curve, and SNR the signal-to-noise ratio. The performances were evaluated for SNR ranging from infinity to 15 dB, therefore covering the values commonly encountered in clinical practice. For each value of the SNR, the normalized mean absolute error ($NMAE$) and its standard deviation (σ_{NMAE}) were calculated for each parameters (κ and k_{ep}), and taken as a measure of estimation accuracy and precision, respectively.

Furthermore, the time performances of the two methods were evaluated by calculating the average computation time needed to fit one CTC.

Parameter estimation was performed by combining a grid search with an iterative loop. More in detail, the parameter t_0 is estimated by a grid search with a resolution of 2 sec. For each t_0 in the grid, a non-linear least square iterative search with the Trust-Region Reflective method is performed to estimate the rest of the parameters [10]. Finally the best fit is chosen according to the least square error criterion. All the analysis is implemented in MATLAB®(MathWorks Inc., Natick, MA) running on a standard PC.

B. Clinical Evaluation

Five patients referred for radical prostatectomy underwent a DCE-MRI exam at the Academic Medical Center (AMC), University of Amsterdam (the Netherlands). All the included patients signed informed consent. After intravenous injection of 0.1 mmol/Kg bolus of Gadobutrol (Gadovist, Bayer), imaging was performed with a 1.5 T MRI scanner (Magnetom Avanto, Siemens) equipped with a transrectal coil, and using a spoiled gradient echo recall sequence with phase oversampling. The sequence settings were TR/TE/flip angle = 50 ms/3.9 ms/70 degrees, the voxel size was 1.67x1.67x4 mm^3, and the time resolution was 3.1 s/volume (for 7 slices). The number of frames acquired was 60 in 3 patients, and 80 in 2 patients.

To enable quantification, the native T_1 relaxation maps were calculated for each patient with an inversion recovery sequence, and the time intensity curves measured with DCE-MRI were converted to concentration-time curves (CTCs), following the procedure in [17].

The clinical validation of the proposed method was performed by comparing the parametric images with the histological analysis of resectioned prostate. The histology specimens used for this study were obtained from patients with proven PCa and analyzed at the AMC. Histological analysis was performed on 4-mm slices, where cancerous tissue was marked by a pathologist based on the microscopic analysis of cell differentiation (Fig. 1e). In order to evaluate the ability of the estimated parameters to diagnose cancer, the marked regions were overlapped to the corresponding MRI parametric maps (Fig. 1a-d). The classification performance of the estimated parameters was evaluated on a voxel level in a total of 29 MRI slices in terms of sensitivity, specificity, and area under the receiving operator characteristic (ROC) curve. Based on the ROC curves, the optimal classification threshold for each parameter was chosen as the point closest to the top-left corner, and sensitivity and specificity were calculated accordingly.

IV. RESULTS

A. Simulations

Table I reports the results of the simulations in terms of *NMAE* and its standard deviation σ_{NMAE} for different SNRs. Regarding the time performance, the average computation time needed to fit one CTC was 1.09 s and 0.61 s with the original and novel method, respectively. Therefore, a reduction of 41% of the computation time was obtained with the novel method.

TABLE I

NORMALIZED MEAN ABSOLUTE ERROR AND STANDARD DEVIATION ($NMAE \pm \sigma_{NMAE}(\%)$)

SNR (dB)	κ (original)	k_{ep} (original)	κ (novel)	k_{ep} (novel)
10000	0.62±3.48	0.33±1.15	0.43±2.09	0.26±0.56
35	1.28±5.20	0.36±1.06	1.13±4.61	0.29±0.55
30	1.46±5.60	0.44±1.20	1.13±4.22	0.34±0.55
25	2.12±7.55	0.53±1.22	1.76±5.80	0.46±0.74
20	2.81±8.69	0.85±1.54	2.48±7.16	0.76±1.08
15	3.64±10.87	1.35±2.04	3.03±8.48	1.17±1.52

B. Clinical Evaluation

The results of the clinical validation are reported in Table II. Classification is evaluated at a voxel level in terms of specificity, sensitivity, and ROC curve area. The average computation time needed to fit one CTC was 1.53 s and 0.96 s for the original and novel method, respectively. Therefore, a reduction of 37% of the computation time was obtained with the novel method.

TABLE II

CLASSIFICATION RESULTS

Parameter	Sensitivity	Specificity	ROC area
k_{ep} (original)	85%	92%	0.92
κ (original)	71%	61%	0.68
k_{ep} (novel)	85%	91%	0.92
κ (novel)	80%	56%	0.72

V. DISCUSSION AND CONCLUSIONS

A novel formulation of the MRDI method for quantitative assessment of tumor angiogenesis is proposed and tested in PCa. The new formulation is obtained by providing an analytical solution for the convolution integral present in the dispersion model.

The convolution integral introduces at each iterative step of the fitting routine N^2 multiplications, where N is the number of time samples in the CTC. Therefore, the asymptotic algorithm complexity of the original MRDI method is $O(N^2)$. By providing a closed-form solution for the convolution integral, the novel MRDI method allows reducing the asymptotic algorithm complexity to $O(N)$, as can be observed in Fig. 1f.

As a result, a reduction by about 40% of the average computation time was achieved with the novel method, without significant changes in the estimation precision and accuracy, evaluated by dedicated simulations, and in the clinical performance, evaluated in five patients.

Although this preliminary validation was performed in PCa, the proposed method can be extended to any form of cancer in which angiogenesis plays an important role.

As new solutions are continuously developed that boost the spatiotemporal resolution of DCE-MRI loops, the number of voxels and of time frames in the DCE-MRI images increases, making the advantages of the proposed solution even more attractive.

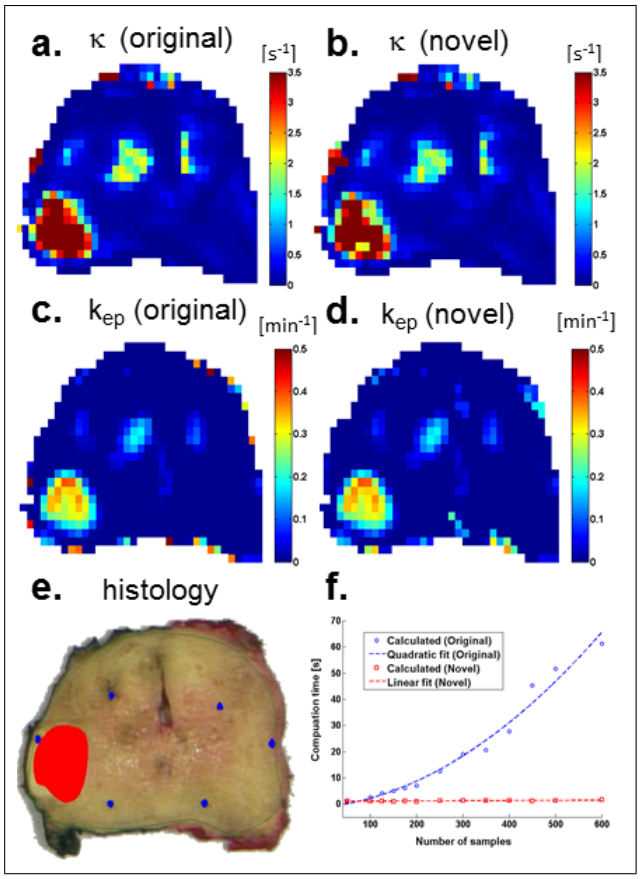

Fig. 1. **a-d**. Parametric maps of κ and k_{ep} obtained with the original (a,c) and novel (b,d) method; **e**. Histology specimen corresponding to the parametric maps in a-d; **f.** Computation time dependency on the number of samples for the original method (blue) and novel method (red).

APPENDIX

The derivation of (6) is here explained more in detail. By expressing (5) as

$$C_t(t-t_0) = A\int_{t_0}^{t+t_0} \sqrt{\frac{\kappa}{2\pi(\tau-t_0)}} e^{-\frac{\kappa(\tau-\mu-t_0)^2}{2(\tau-t_0)}} e^{-k_{ep}(t-\tau)} d\tau, \tag{8}$$

and making the substitution $\tau - t_0 = \sigma$, equation (5) can be rewritten as

$$C_t(t) = A\sqrt{\frac{\kappa}{2\pi}} e^{-k_{ep}(t-t_0+\kappa\mu)} \int_0^t \sqrt{\frac{1}{\sigma}} e^{\left(\frac{1}{2}\kappa - k_{ep}\right)\sigma - \frac{\kappa\mu^2}{\sigma}} d\sigma. \tag{9}$$

Then, with the substitution $\sigma = x^2$, equation (9) becomes

$$C_t(t) = 2A\sqrt{\frac{\kappa}{2\pi}} e^{-k_{ep}(t-t_0+\kappa\mu)} \int_0^{\sqrt{t}} e^{\left(\frac{1}{2}\kappa - k_{ep}\right)x^2 - \frac{\kappa\mu^2}{x^2}} dx. \tag{10}$$

The integral in (10) can be solved by using the known integral in [18], given below

$$\int_0^x e^{-a^2x^2 - \frac{b^2}{x^2}} dx = \frac{\sqrt{\pi}}{4a}[e^{2ab}(erf(ax+b/x)-1) + e^{-2ab}(erf(ax-b/x)+1)]. \tag{11}$$

In fact, by making the change of variables in (7), the integral in (10) can be written as

$$\int_0^{\sqrt{t}} e^{\left(\frac{1}{2}\kappa - k_{ep}\right)x^2 - \frac{\kappa\mu^2}{x^2}} dx = \int_0^{\sqrt{t}} e^{-zx^2 - \frac{\varpi}{x^2}} dx. \tag{12}$$

Therefore, equation (12) can be solved using (11), leading to the solution given in (6).

REFERENCES

[1] P. Camerliet, "Angiogenesis in life, disease and medicine," *Nature*, vol. 438, no. 15, pp. 932–936, 2005.

[2] G. Russo, M. Mischi, W. Scheepens, J. J. de la Rosette, and H. Wijkstra, "Angiogenesis in prostate cancer: onset, progression and imaging," *BJU International*, vol. 110, no. 11c, pp. E794–E808, 2012.

[3] H.-C. Wu, C.-T. Huang, and D.-K. Chang, "Anti-angiogenic therapeutic drugs for treatment of human cancer," *Journal of Cancer Molecules*, vol. 4, no. 2, pp. 37–45, 2008.

[4] A. Tefekli and M. Tunc, "Future prospects in the diagnosis and management of localized prostate cancer," *The Scientific World Journal*, vol. 2013, p. 9, 2013.

[5] G. Bozzini, P. Colin, P. Nevoux, A. Villers, S. Mordon, and N. Betrouni, "Focal therapy of prostate cancer: energies and procedures," *Urol Oncol-Semin Ori*, vol. 31, no. 2, pp. 155–167, 2013.

[6] T. Jeswani and R. Padhani, "Imaging tumour angiogenesis," *Cancer Imaging*, vol. 5, pp. 131–138, 2005.

[7] G. Brix, J. Griebel, F. Kiessling, and F. Wenz, "Tracer kinetic modelling of tumour angiogenesis based on dynamic contrast-enhanced ct and mri measurements," *Eur J Nucl Med Mol Imaging*, vol. 37, pp. S30–S51, 2010.

[8] B. Turkbey, H. Kobayashi, M. Ogawa, M. Bernardo, and P. Choyke, "Imaging of tumor angiogenesis: Funcional or targeted?" *Am J Roengtenol*, vol. 193, pp. 304–313, 2009.

[9] M. P. J. Kuenen, M. Mischi, and H. Wijkstra, "Contrast-ultrasound diffusion imaging for localization of prostate cancer," *IEEE T Med Imaging*, vol. 30, no. 8, pp. 1493 – 1502, 2011.

[10] M. Mischi, T. Saidov, K. Kompatsiari, M. R. W. Engelbrecht, M. Breeuwer, and H. Wijkstra, "Prostate cancer localization by novel magnetic resonance dispersion imaging," in *Engineering in Medicine and Biology Society (EMBS), 2013 35th Annual International Conference of the IEEE*, Conference Proceedings, pp. 2603–2606.

[11] P. S. Tofts, G. Brix, D. L. Buckley, J. L. Evelhoch, E. Henderson, M. V. Knopp, H. B. Larsson, T.-Y. Lee, N. A. Mayr, G. J. Parker, R. E. Port, J. Taylor, and R. M. Weisskoff, "Estimating kinetic parameters from dynamic contrast-enhanced t1-weighted mri of a diffusable tracer: Standardized quantities and symbols," *J Magn Reson Im*, vol. 10, no. 3, pp. 223–232, 1999.

[12] R. Siegel, J. Ma, Z. Zou, and A. Jemal, "Cancer statistics, 2014," *CA-Cancer J Clin*, vol. 64, no. 1, pp. 9–29, 2014.

[13] H. Wijkstra, M. Wink, and J. J. de la Rosette, "Contrast specific imaging in the detection and localization of prostate cancer," *World J Urol*, vol. 22, no. 5, pp. 346–350, 2004.

[14] T. Franiel, B. Hamm, and H. Hricak, "Dynamic contrast-enhanced magnetic resonance imaging and pharmacokinetic models in prostate cancer," *Eur Radiol*, vol. 21, no. 3, pp. 616–626, 2011.

[15] K. S. S. Lawrence and T.-Y. Lee, "An adiabatic approximation to the tissue homogeneity model for water exchange in the brain: I. theoretical derivation," *J Cereb Blood Flow Metab*, vol. 18, no. 12, pp. 1365–1377, 1998.

[16] A. S. N. Jackson, S. A. Reinsberg, S. A. Sohaib, E. M. Charles-Edwards, S. Jhavar, T. J. Christmas, A. C. Thompson, M. J. Bailey, C. M. Corbishley, C. Fisher, M. O. Leach, and D. P. Dearnaley, "Dynamic contrast-enhanced mri for prostate cancer localization," *Brit J Radiol*, vol. 82, no. 974, pp. 148–156, 2009.

[17] M. C. Schabel and D. L. Parker, "Uncertainty and bias in contrast concentration measurements using spoiled gradient echo pulse sequences," *Phys Med Biol*, vol. 53, no. 9, p. 2345, 2008.

[18] A. Prudnikov, A. Brychkov, and O. Marichev, *Integrals and series, Vol.1: Elementary functions.* NY: Gordon and Breach, 1986, book section 1.3.3.20.